Journal of Statistical Physics, Vol. 53, Nos. 3/4, 1988

Vibrational Properties of Hierarchical Systems

W. P. Keirstead,[1] H. A. Ceccatto,[2] and B. A. Huberman[3]

Received March 30, 1988; revision received May 11, 1988

The vibrational properties of one-dimensional hierarchical systems are investigated and results are obtained for both their eigenvalues and eigenvectors. Two cases are considered, the first one with a hierarchy of spring constants and the latter with a hierarchy in the masses. In both cases the eigenspectrum is found to be a zero-measure, two-scale Cantor set with a fractal dimension between 0 and 1. The scaling properties of the spectra are calculated using renormalization group techniques and are verified by extensive numerical work. The low-frequency density of states and low-temperature specific heat are calculated and a singularity is found in the scaling behavior. The eigenvectors are found to be either extended or critical and self-similar. A transfer matrix formalism is introduced to calculate the scaling properties of the envelope of the critical eigenvectors. Furthermore, a connection is established between the hierarchical vibration and diffusion problems, as well as to the same problems in random systems, thus showing the universality of the observed features.

KEY WORDS: Hierarchical systems; phonons; Cantor spectra; renormalization group.

1. INTRODUCTION

Complex physical structures very often display a hierarchical organization. This is reflected in the large span of characteristic times with which they respond to external perturbations. A large molecule with different force constants, for example, might exhibit a vibrational spectrum that reflects the effective decoupling of low- and high-frequency components. This can lead in turn to complicated spectra which when measured could be used to elucidate the underlying structure of the system.

[1] Physics Department, Stanford University, Stanford, California 94305.
[2] Applied Physics Department, Stanford University, Stanford, California 94305.
[3] Xerox Palo Alto Research Center, Palo Alto, California 94304.

0022-4715/88/1100-0733$06.00/0

Recently, much attention has been devoted to the transport[1-5] and electronic[6-10] properties of hierarchical systems. In the case of diffusion, it has been shown that a hierarchical arrangement of energy barriers can give rise to anomalous behavior, i.e., the mean-squared displacement $\langle r^2(t) \rangle \sim t^{x(R)}$, where the exponent x can take on values anywhere between 0 and the normal value of 1. Furthermore, the exponent x is found to undergo a phase transition as the parameter R characterizing the hierarchy (equivalent to the temperature in this case) is varied. In the quantum Schrödinger problem, the eigenspectrum is found to be a zero-measure Cantor set and the eigenstates self-similar and critical. In this paper we study another aspect of the hierarchical systems, namely their vibrational properties. In the context of random[11,12] or quasiperiodic[13,14] systems, the vibrational problem has had a long history. In the hierarchical problem, the vibrational spectrum is unknown, and it is the purpose of this paper to elucidate its nature.

We begin our investigation in Section 2 with a basic description of the problem and the fundamental equations involved. We treat two distinct cases, a first one with a hierarchy in the values of the spring constants and all the masses identical, and a second with a hierarchy in the masses and a fixed value for the spring constants. We also consider, as a simple example, a system where all masses and spring constants are the same, the results of which will prove a convenient reference point. In Section 3, we solve for the frequency spectrum for the first case above, employing both numerical and analytical techniques. We find that the allowed frequencies form a zero-measure Cantor set and we calculate its fractal dimension. Using a renormalization group procedure, we are able to account for numerically observed scaling properties of the spectrum. In Section 4, we turn to the properties of the eigenvectors in the first case. Numerically, we observe two types of eigenvectors: extended states and critical states (a nonnormalizable state where the envelope of the function decays algebraically from the maximum). We relate these eigenvectors to the appropriate parts of the spectrum observed in Section 3, and for the critical states we calculate the scaling exponent for the envelope using a transfer matrix formalism.

In Section 5, we discuss the frequency spectrum for the second case. We find qualitatively similar results to that found for the first case, and we again present a renormalization group analysis to explain the numerically observed features. In Section 6, we apply the results derived in the previous parts to the calculation of the density of states and heat capacity. We find an anomalous behavior for the exponent of the specific heat ($C \sim T^x$) as well as a singularity in the exponent as the hierarchy parameter R approaches a critical value R_c. We also relate the hierarchical vibration problem to the hierarchical diffusion problem, as well as to both the

random diffusion and random vibration problems, which reveals the universality of the properties we have found. In Section 7, we summarize our results and making a few closing comments.

2. STATEMENT OF THE PROBLEM

We consider a one-dimensional chain with neighboring masses connected by springs. Letting x_n denote the displacement from equilibrium of the nth mass, and assuming that $x_n(t) = x_n e^{-i\omega t}$, Newton's law gives the basic equation of motion (written in an appropriate dimensionless form):

$$-m_n\omega^2 x_n = k_{n,n+1}(x_{n+1} - x_n) + k_{n-1,n}(x_{n-1} - x_n) \tag{2.1}$$

The spring contstants are assumed to be symmetric, i.e., $k_{n,n+1} = k_{n+1,n}$. One can identify two distinct cases to study. In the first case (case I), we put the hierarchy in the spring constants, while keeping the values of the masses fixed. Explicitly, this means that we set $m_n \equiv 1$, and take the spring constants to be given by

$$k_{n-1,n} = k_{j(n)} = R^{j(n)} \qquad \text{(Case I)} \tag{2.2}$$

where $j(n)$ is the largest power of 2 which divides n. Here, R is some dimensionless parameter, which we will assume for simplicity lies in the interval $[0, 1]$. We have represented schematically the hierarchy of spring constants in Fig. 1a. In Sections 3 and 4 we will solve for the eigenvalues and normal mode eigenvectors of Eq. (2.1) under these conditions.

In the second case (case II), we take the hierarchy to be in the masses and keep the spring constants fixed. Thus, we take $k_{n-1,n} \equiv 1$, and assume that the masses are given by

$$m_n = \mu_{j(n)} = R^{j(n)} \qquad \text{(Case II)} \tag{2.3}$$

where $j(n)$ is again the largest power of 2 which divides n. For convenience, we take R to be in the interval $[1, \infty)$ here. Figure 1b gives a schematic representation of the distribution of masses in this case. In Section 5, we will discuss the eigenvalue solutions to Eq. (2.1) for this case.

One should note that the hierarchies described by Eqs. (2.2) and (2.3) are not the only possibilities. Instead of these simple binary structures, one might consider n-ary ones or even "complex" ones (in the sense of Huberman and Hogg).[15-17] We claim, however, that the general features of the results we obtain here are reproduced in these other systems. We choose the binary case because it lends itself to a simple renormalization group treatment.

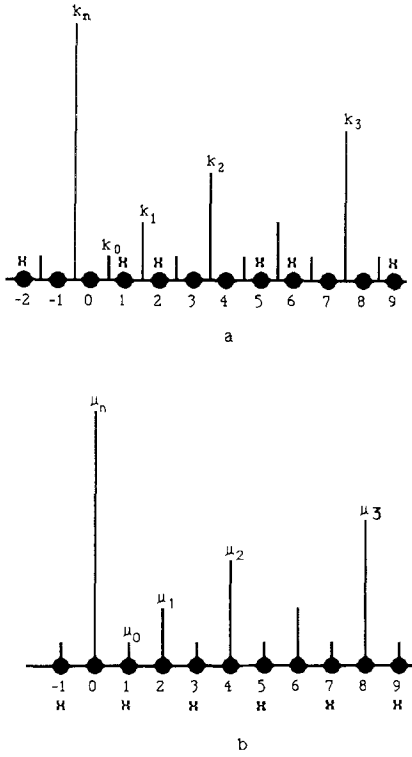

Fig. 1. (a) Schematic representation of the hierarchy of spring constants in case I. A dot represents a mass and the height of a line between two neighboring masses determines the spring constant value k. Note that the drawing is for $R > 1$, although we consider the case $R < 1$ in the text. The "x" marks denote those cells which are decimated in the renormalization described in Section 3.2. (b) Schematic representation of the hierarchy of mass values in case II. A dot represents a mass site, the height of a line above any mass determines its value μ, and the "x" marks denote those masses which are decimated in the renormalization described in Section 5.2.

Before proceeding to the solution of the above cases, it is instructive to consider first the case where both the spring constant and mass values are fixed, i.e., the $R \to 1$ limit of cases I and II above. Here, we make use of the unit periodicity to label the eigenstates by a wavevector q. Then we have $x_{n+j} = x_n e^{iqj}$. Applying this to Eq. (2.1) gives the dispersion relation

$$\omega^2 \equiv z = 4 \sin^2 q/2 \tag{2.4}$$

Thus, the allowed squared vibrational frequencies z (it will be convenient to use z instead of ω) lie in the interval $[0, 4]$. The eigenvectors are given by $x_n(q) = x_0 e^{iqn}$ and are clearly extended states.

3. VIBRATIONAL SPECTRUM. CASE I

3.1. Numerical Results

We begin our study of the vibrational spectrum of Eq. (2.1) under the conditions of Eq. (2.2) by considering some numerical results. We choose to study the infinite hierarchical system by considering it as the limit of a sequence of periodic systems of size $p_n = 2^n$, $n = 1, 2, \ldots$. The period p_n system is obtained from Eq. (2.2) by setting all spring constants k_j, $j \geqslant n$, equal to k_n. Thus, the period p_n system has precisely n distinct spring constants. Because of the periodicity, we may label the eigenvectors by a wavevector q such that $x_{j+p} = x_j e^{iqp}$. Applying this to Eq. (2.2), we see that for any value of $q \in [0, 2\pi]$ we may reduce the infinite set of equations to a set of p_n equations. Thus, we will generate p_n bands of allowed frequencies. Clearly, each band contains the same number of states (a finite number if one includes boundary conditions on the system so as to quantize q). The band edges will occur when $q = 0$ or $q = \pi$. If we numerically diagonalize the above p_n equations, with q taking on these two values, we will solve for the $2p_n$ edges of the p_n bands. The resulting band structure can then be investigated.

We have carried out this numerical procedure for several different combinations of period and R. Figure 2 shows an example of the band structures one obtains at a fixed value of R for a series of systems of

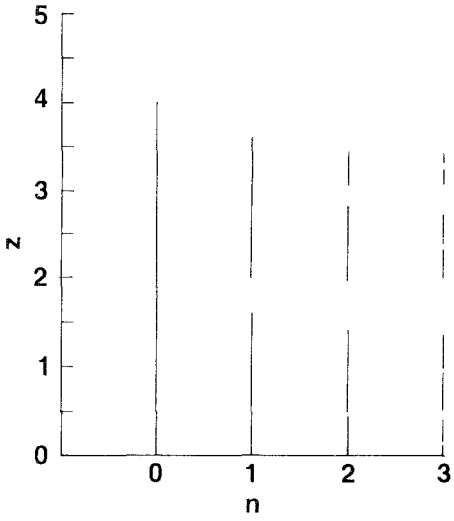

Fig. 2. The allowed frequency bands (in dimensionless units) in case I for periodic systems of period 2^n, $n = 0, 1, 2, 3$. We have used $R = K = 0.8$.

increasing period. From analysis of the numerical results, we find that the total bandwidth B_n of the period p_n system behaves exactly as

$$B_n = 4R^n \tag{3.1}$$

This fact, along with the development of the band structure with increasing period (as shown in Fig. 2), reveals that the allowed frequency spectrum of the infinite system forms a Cantor set of zero Lebesgue measure (we define a Cantor set to be a closed set containing no interior or isolated points). Hence, the spectrum is a fractal or, as we shall see, a multifractal set.

It is of interest to characterize the various properties of the spectrum, and in particular to investigate the scaling behavior of the band splittings and to calculate the fractal (or Hausdorff) dimension of the set. An examination of Fig. 2 reveals a great deal of self-similarity in the structure of the bands as we keep doubling the period. We see that every band splits into two bands as the period of the system is doubled. Furthermore, by studying the numerical results for a number of different cases, we find that there are two scaling parameters that describe the sequence of band splittings for a particular R value: the first characterizes the limiting ratio of the bandwidth of a band in the period p_n system to the bandwidth of the lower band into which it splits for the period p_{n+1} system; the second characterizes the ratio with respect to the upper band into which it splits. For example, for $R = 0.2$, we find that the first scaling parameter is $\lambda_1 \approx 10.00$, and the second scaling parameter is $\lambda_2 \approx 12.17$. For $R = 0.8$, we find $\lambda_1 \approx 4.00$ and $\lambda_2 \approx 4.98$. Hence, we clearly see that the frequency spectrum of the infinite system is a two-scale Cantor set.

From the above numerical information, we may also determine the fractal dimension D_0 of the set. If we define $N(n, l)$ to be the number of segments of length l which it takes to cover the bands of the period p_n system, then by definition $N(n, l) \sim l^{-D_0}$. The total bandwidth then scales as $B_n \sim l^{-D_0}$. But from the above, we know that $B_n \sim R^n$ and $N(n, l) \sim 2^n$. Combining these expressions gives

$$D_0 = \log 2/\log(2/R) \tag{3.2}$$

There is another interesting property of the spectrum worth noting. Consider, for instance, the p_n bottom band edge values in the period p_n system. Note that for all larger period systems, these values remain at the bottom edges of various bands. Hence, these points are in the spectrum of the infinite system. (They are not the only points in the spectrum because there are only a countable number of them, while the spectrum is uncountable). The same is not true for the upper band edges: we clearly see that their values are not preserved when the period size increases.

3.2. Renormalization Group Treatment

We now provide a concrete analytical understanding of the above numerical results. We do so by considering a renormalization of the original equations of motion. We choose to decimate all cells marked with an "x" in Fig. 1a; that is, we eliminate all x_n, where $n = 4j + 1$ or $n = 4j + 2$, in terms of the remaining variables. For cells $-1, 0, \ldots, 3$, we have

$$\begin{aligned}(k_0 + k_1 - z)\, x_1 &= k_1 x_2 + k_0 x_0 \\ (k_0 + k_1 - z)\, x_2 &= k_0 x_3 + k_1 x_1\end{aligned} \tag{3.3}$$

Thus, our equation for x_0 becomes

$$\begin{aligned}(k_n + k_0 - z)\, x_0 &= k_n x_{-1} + k_0 x_1 \\ &= k_n x_{-1} + k_0 \left[\frac{k_0 (k_0 + k_1 - z)}{\Delta} x_0 + \frac{k_0 k_1}{\Delta} x_3 \right]\end{aligned} \tag{3.4}$$

where $\Delta = (k_0 + k_1 - z)^2 - k_1^2$. We recast this equation in a form so as to make the renormalized system resemble the original as much as possible:

$$-z' x'_{0'} = k'_{n-1}(x'_{-1'} - x'_{0'}) + k'_0 (x'_{1'} - x'_{0'}) \tag{3.5}$$

where the renormalized spring constants, frequency, and eigenvector are given by

$$\begin{aligned} k'_0 &= k_0 \\ k'_{n-1} &= \frac{\Delta}{k_0 k_1} k_n, \qquad n \geqslant 2 \\ z' &= \frac{(z - k_0)\Delta + k_0^2 (k_0 + 2k_1 - z)}{k_0 k_1} \\ x'_{n'} &= x_{\lfloor n/2 \rfloor} \end{aligned} \tag{3.6}$$

Here, $\lfloor n/2 \rfloor$ denotes the greatest integer less than or equal to $n/2$. Note in particular that the magnitude of the eigenvector is not renormalized, only the labeling of the components changes.

Let us now generalize the definition of the spring constants given in Eq. (2.2), by assuming that

$$k_n = \begin{cases} 1 & \text{if } n = 0 \\ KR^{n-1} & \text{otherwise} \end{cases} \tag{3.7}$$

If we set $K=R$, we obtain Eq. (2.2). This generalization will allow us to write the renormalization equations (3.6) in terms of two parameters only (not counting the trivial renormalization of the eigenvector indices), namely K and z. In particular, we obtain

$$K' = R\Delta$$
$$z' = \frac{(z-1)\Delta + (1+2K-z)}{K} \tag{3.8}$$

We now have $\Delta = (1+K-z)^2 - K^2$. The other renormalized spring constants are $k'_0 = 1$ and $k'_n = K'R^{n-1}$, $n \geqslant 1$.

We may now make use of this two-parameter renormalization to classify the allowed frequencies. Let us treat the infinite system as a periodic one with period p_n for some very large n. Initially, we have $K \equiv K^{(0)} = R$, and we wish to determine whether some frequency $z \equiv z^{(0)}$ is in the spectrum. We note that each application of Eqs. (3.8) reduces the period of the system by a factor of two and renormalizes the values of K and z. After $n-1$ such steps, we will have a system of period $p_1 = 2$. Suppose that we know the allowed frequencies for the period-two system for an arbitrary value of K (we will derive this momentarily). Then we have the following condition: $z^{(0)}$ is in the spectrum of the period-p_n system provided $z^{(n-1)}$ is in the spectrum of the period-two system.

Because of the role played by the period-two system in the above argument, let us derive its band structure for an arbitrary spring constant K. Define the transfer matrix M_1 such that

$$\begin{pmatrix} x_{2n+1} \\ x_{2n} \end{pmatrix} = M_1^n \begin{pmatrix} x_1 \\ x_0 \end{pmatrix} \tag{3.9}$$

Using $k_0 = 1$ and $k_1 = K$, we may explicitly determine M_1 as

$$M_1 = \frac{1}{K}\begin{pmatrix} \Delta & -(1+K-z) \\ (1+K-z) & -1 \end{pmatrix} \tag{3.10}$$

We require that x_n remain bounded as $n \to \infty$. Defining $T_1 = \operatorname{Tr} M_1$, we must have

$$|T_1| = \left| \frac{\Delta - 1}{K} \right| \leqslant 2 \tag{3.11}$$

Equation (3.11) leads to the presence of two bands: for $K \leqslant 1$, the lower band has $0 \leqslant z \leqslant 2K$, and the upper has $2 \leqslant z \leqslant 2 + 2K$. Note that this result agrees with the period-two structure seen in Fig. 2 (setting $K = R$).

The condition expressed by Eq. (3.11) applied to $z^{(n-1)}$ and $K^{(n-1)}$ determines whether or not z is in the spectrum of the period-p_n system. For the infinite system, then, we need to investigate the behavior of these iterates as $n \to \infty$. We do so by examining the fixed points of Eqs. (3.8). A short calculation reveals the existence of two fixed points:

$$K_1^* = \begin{cases} R/(1-2R), & 0 \leqslant R \leqslant 1/2, \\ +\infty, & 1/2 \leqslant R \leqslant 1, \end{cases} \qquad z_1^* = 0 \tag{3.12}$$

$$K_2^* = \frac{R}{1-R^2}, \qquad z_2^* = \frac{2-R}{1-R} \tag{3.13}$$

If we evaluate T_1 at these fixed points, we find $T_1^{(1)*} = 2$ and $T_1^{(2)*} = R$. Thus, initial frequencies which iterate to one of these fixed points are in the spectrum, and hence both of them are relevant to the problem.

Next, we examine the scaling properties of these fixed points. Evaluating the matrix of partial derivatives $[\partial(z', K')/\partial(z, K)]$ at the two fixed points and diagonalizing, we find the eigenvalues

$$\lambda_{1,2}^{(1)} = \begin{cases} 2R^{\mp 1}, & 0 \leqslant R \leqslant 1/2 \\ 4, 2R, & 1/2 \leqslant R \leqslant 1 \end{cases} \tag{3.14}$$

$$\lambda_{1,2}^{(2)} = \frac{1}{2R}\{(2+2R+R^2) \pm [(2+2R+R^2) - 8R^3]^{1/2}\} \tag{3.15}$$

We note that in both cases (and for any value of R) $\lambda_{\max} > 1$, and hence both fixed points are unstable. This is consistent with the Cantor set property of the system we discovered above. Furthermore, we may relate these eigenvalues to the scaling properties of the spectrum, as seen in Fig. 2. Numerical investigation of large-period systems reveals that points near the lower edge of any band are attracted initially toward the first fixed point before eventually veering away (with the exception of the point $z = 0$, for which all iterates $z^{(n)}$ are zero); points near the upper edge of any band are initially attracted toward the second fixed point. Thus, $\lambda_{\max}^{(1)}$ should be the relevant scaling parameter for the evolution of the lower-band splitting and $\lambda_{\max}^{(2)}$ that for the upper-band splitting. For $R = 0.2$, we find $\lambda_{\max}^{(1)} = 10$ and $\lambda_{\max}^{(2)} = 12.1671\ldots$. For $R = 0.8$, we get $\lambda_{\max}^{(1)} = 4$ and $\lambda_{\max}^{(2)} = 4.9786\ldots$. These numbers are in excellent agreement with those found numerically above.

Lastly, we can account for the numerical observation that the bottom band edges (see Fig. 2) for any of the periodic systems are also in the spectra of all larger-period systems, in particular of the infinite system. Consider the values of z which iterate to $z_1^* = 0$ in $n-1$ steps, assuming $K = R$ initially (K will also iterate to K_1^*, although not in a finite number of

steps). We find that there are precisely p_n solutions and that they are equal to the observed lower band edges for the period-p_n system. Since $T_1(z=0, K)=2$, for any K, and since $z=0$ iterates to itself upon renormalization, we see that these points will remain in the spectra of all the larger-period systems.

4. NATURE OF THE EIGENVECTORS. CASE I

The next question we address is the nature of the eigenvectors of Eq. (2.1) in case I. We begin by considering a generalization of the transfer matrix method introduced in Section 3.2 for the period-two system. Knowledge of the transfer matrices enables us to determine the value of the eigenvector at any site. In particular, we will be interested in the shape of the envelope of the eigenvectors. We find two basic types: the first one has a constant magnitude and hence corresponds to an extended state, while the second shows algebraic decay of the envelope from the maximum and is thus a critical state. These results are verified by numerical work.

4.1. Transfer Matrix Formalism

Let us define the two-vector $\mathbf{x}_j=(x_{j+1}, x_j)^T$. We may then define the 2×2 transfer matrix M_n by (recall that $p_n=2^n$)

$$\mathbf{x}_{p_n}=M_n\mathbf{x}_0 \tag{4.1}$$

If we also define B_n such that $\mathbf{x}_{p_n}=B_n\mathbf{x}_{p_n-2}$, then we can easily see that

$$M_n\equiv\begin{pmatrix}\alpha_n & \beta_n\\ \gamma_n & \delta_n\end{pmatrix}=A_nM_{n-1}^2 \tag{4.2}$$

where $A_n=B_nB_{n-1}^{-1}$. The expression for M_1 is given in Eq. (3.10). A tedious but straightforward calculation then leads to the following expression for A_n:

$$A_n=f_nC+I \tag{4.3}$$

where $f_n=(1-R)/(KR^{n-1})$, $\mu=z-1$, I is the 2×2 identity matrix, and C is given by

$$C=\begin{pmatrix}-\mu & -\mu^2\\ 1 & \mu\end{pmatrix} \tag{4.4}$$

The transfer matrix has a number of properties which may be deduced from the above expressions. First, note from Eqs. (4.3) and (3.10) that

$\det A_n = \det M_1 = 1$. Thus, from Eq. (4.2) we see that $\det M_n = 1$ for every n. Second, knowledge of the transfer matrices and the values of the eigenvector in two cells (typically cells 0 and 1), which are determined by the global boundary conditions and normalization, is sufficient to determine the value of the eigenvector in any cell. For example, suppose the values x_0 and x_1 are known, and we wish to find x_{26}. Note that $26 = 2^4 + 2^3 + 2^1$, hence x_{26} is given by the upper component of the two-vector $M_1 M_3 M_4 \mathbf{x}_0$. A similar binary decomposition will work for any other cell.

Next, we may use the transfer matrix M_n to determine the allowed frequencies for the period-p_n system. From Eq. (4.1), we see that boundedness of the eigenvector components requires that $|T_n| \leqslant 2$, where $T_n \equiv \operatorname{Tr} M_n$. This condition clearly must be equivalent to that derived in Section 3, where we found that z is in the spectrum of the period-p_n system with spring constant K if and only if its iterate $z^{(n-1)}$ is in the period-two system with renormalized spring constant $K^{(n-1)}$. Hence, we conclude that $T_n(z, K) = T_1(z^{(n-1)}, K^{(n-1)})$. In particular, if (z^*, K^*) is a fixed point, then $T_n(z^*, K^*) = T_1(z^*, K^*)$ regardless of n. Equation (3.11) gives the exact value for this trace.

Equation (4.2) is a nonlinear matrix equation and is difficult to solve for general values of z and K. However, at either of the two fixed points given by Eqs. (3.12) and (3.13), we may linearize the recursion relation for M_n and solve the resulting equation exactly. This enables us to determine the behavior of the eigenvector at either of the two fixed points. To linearize Eq. (4.2), we first note that for any 2×2 matrix A with determinant 1, $A^2 - A \operatorname{Tr} A + I = 0$. Now, M_{n-1} is such a matrix, where $\operatorname{Tr} M_{n-1}(z^*, K^*) = \operatorname{Tr} M_1(z^*, K^*) \equiv t$. (It is crucial to note that t is independent of n here; this is what makes the linearization possible at the fixed points.) Thus, Eq. (4.2) gives

$$M_n = A_n(tM_{n-1} - I) \tag{4.5}$$

To solve Eq. (4.5), we note that the product of two of the A matrices can be written as

$$\begin{aligned} A_i A_j &= (f_i C + I)(f_j C + I) \\ &= f_i f_j C^2 + (f_i + f_j) C + I \\ &= (f_i + f_j) + I \end{aligned} \tag{4.6}$$

since the $C^2 = 0$. We may now iterate Eq. (4.5) to write M_n in terms of M_1 and products of A matrices:

$$M_n = t^{n-1}(A_n A_{n-1} \cdots A_2) M_1 - \sum_{j=0}^{n-2} t^j (A_n A_{n-1} \cdots A_{n-j}) \tag{4.7}$$

The products of the A matrices may be evaluated by repeated use of Eq. (4.6). We obtain

$$A_n A_{n-1} \cdots A_{n-j} = (f_n + f_{n-1} + \cdots + f_{n-j})C + I$$
$$= \frac{1 - R^{j+1}}{KR^{n-1}} C + I \tag{4.8}$$

If we now insert Eq. (4.8) into Eq. (4.7), sum all the resulting geometric series, and multiply out the matrices, we arrive at the following expressions for the components of M_n:

$$\begin{aligned}
\alpha_n &= \frac{1}{K}\left(\frac{t}{R}\right)^{n-1}(1-z)^2 \\
&\quad + \left[2t^{n-1} + \frac{1}{KR^{n-1}}\left(R\frac{1-(tR)^{n-1}}{1-tR} - \frac{1-t^{n-1}}{1-t}\right)\right](1-z) \\
&\quad - \frac{1-t^{n-1}}{1-t} \\
\beta_n &= -\frac{1}{K}\left(\frac{t}{R}\right)^{n-1}(1-z) - t^{n-1} \\
&\quad - \frac{1}{KR^{n-1}}\left[R\frac{1-(tR)^{n-1}}{1-tR} - \frac{1-t^{n-1}}{1-t}\right](1-z)^2 \\
\gamma_n &= \frac{1}{K}\left(\frac{t}{R}\right)^{n-1}(1-z) + t^{n-1} + \frac{1}{KR^{n-1}}\left[R\frac{1-(tR)^{n-1}}{1-tR} - \frac{1-t^{n-1}}{1-t}\right] \\
\delta_n &= -\frac{1}{K}\left(\frac{t}{R}\right)^{n-1} - \frac{1}{KR^{n-1}}\left[R\frac{1-(tR)^{n-1}}{1-tR} - \frac{1-t^{n-1}}{1-t}\right](1-z) \\
&\quad - \frac{1-t^{n-1}}{1-t}
\end{aligned} \tag{4.9}$$

One may check these equations by showing that $\det M_n = 1$, $\operatorname{Tr} M_n = t$ [when evaluated at the fixed points given by Eqs. (3.12) and (3.13)], and that for $n = 1$ they reduce to Eq. (3.10).

Let us now evaluate Eq. (4.9) at the fixed points found in Section 3. Consider first the fixed point (FP1) of Eq. (3.12) for $R < 1/2$. Here, the trace $t = 2$. We may simplify Eq. (4.9) to find

$$M_n = \frac{1-R}{R^n}\begin{pmatrix} 1 & -1 \\ 1 & -1 \end{pmatrix} + I \qquad \text{(FP1, } R < 1/2\text{)} \tag{4.10}$$

For $R > 1/2$, we have

$$M_n = 2^{n-1}\begin{pmatrix} 1 & -1 \\ 1 & -1 \end{pmatrix} + I \qquad \text{(FP1, } R > 1/2\text{)} \tag{4.11}$$

At the second fixed point (FP2), Eq. (3.13), the trace $t = R$ and the transfer matrix reduces to

$$\begin{aligned} \alpha_n &= \frac{1}{1-R}(R^{-n}-1) \\ \beta_n &= R^{-1} + 1 - R^{n-1} + \frac{(R^{-n}-1)(1-R^{n-1})}{(1-R)^2}, \qquad \text{(FP2)} \\ \gamma_n &= -R^{-n} \\ \delta_n &= -R^{-1} + R - \frac{R^{-n}-R^{-1}}{1-R} \end{aligned} \tag{4.12}$$

4.2. Numerical Results

Before applying the results of Section 4.1 to the analysis of the eigenvectors, we first consider some numerical results. To obtain a numerical picture of the eigenvectors at the fixed points, we apply Eq. (2.1) with the appropriate spring constants and frequency to obtain x_j in terms of x_{j-1} and x_{j-2}. We then need only specify the values of x_0 and x_1, say, and all others will follow. To determine x_0 and x_1, let us again treat the infinite system as the limit of a sequence of periodic systems, as in Section 3. For a system of period $p_n = 2^n$, the periodicity permits us to label each eigenvector with a wavevector q such that $x_{n+p_n} = x_n e^{iqp_n}$. Thus, $x_{p_n} = x_0 e^{iqp_n}$. But, from the transfer matrix we have x_{p_n} as the lower component of $M_n \mathbf{x}_0$, i.e., $x_{p_n} = \gamma_n x_1 + \delta_n x_0$. Equating the two expressions, and assuming an overall normalization such that $x_0 = 1$, we find that

$$\begin{aligned} x_1 &= \lim_{n\to\infty} -[(\delta_n - e^{iqp_n})/\gamma_n] \\ &= -\delta_n/\gamma_n \\ &= \begin{cases} 1, & \text{FP1} \\ -1/(1-R), & \text{FP2} \end{cases} \end{aligned} \tag{4.13}$$

We have used these boundary conditions for cells 0 and 1 to plot the eigenvectors at the two fixed points, with typical results shown in Fig. 3. The eigenvector corresponding to FP1 (Fig. 3a) has a constant magnitude

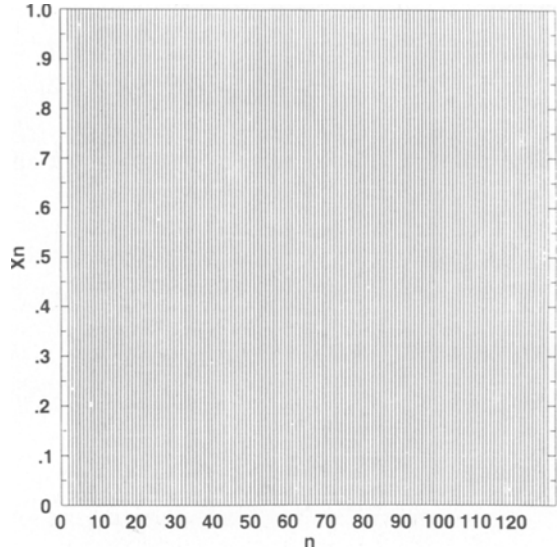

(a)

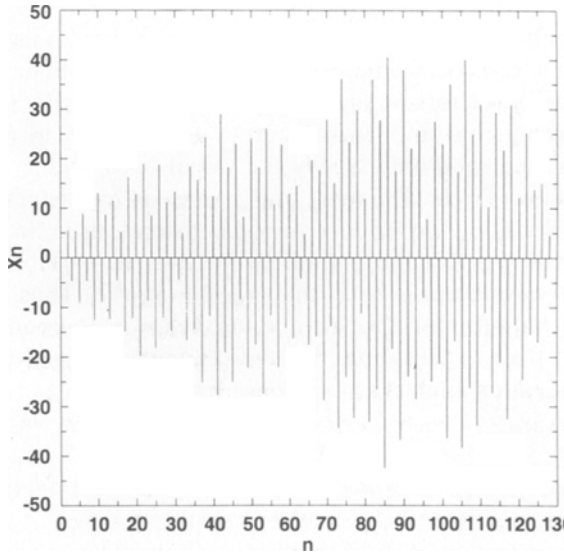

(b)

Fig. 3. (a) The eigenvector in case I corresponding to the first fixed point. We have used $R = K = 0.8$, although any other value of R gives the same picture. (b) The eigenvector in case I corresponding to the second fixed point, plotted for the first 128 cells. We have used $R = K = 0.8$. (c) Same as in (b), except plotted for the first 512 cells. Note the self-similarity.

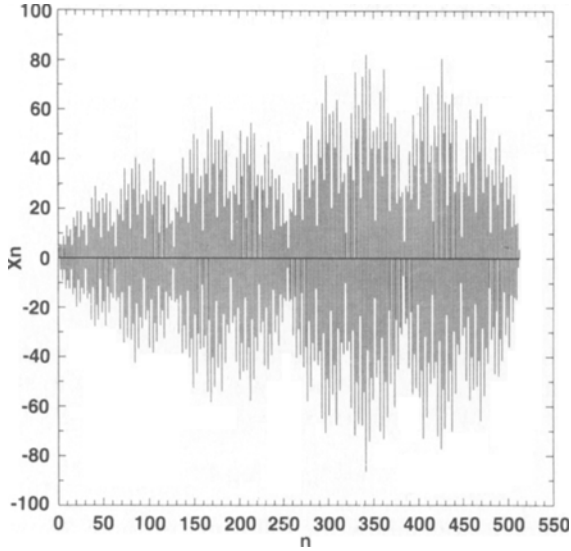

(c)

Fig. 4 (*continued*)

equal to one, and is clearly an extended state. The result is independent of R. This may easily be seen from Eq. (2.1) when $z^* = 0$. In that case, we have $x_n = x_1 = 1$ for any n.

The eigenvector for the second fixed point (Figs. 3b and 3c) is more interesting. It is self-similar, as is apparent in the diagrams. It also increases in magnitude, although not monotonically, as one moves away from the origin. If we identify the maxima within any given "bicade," i.e., the region between cells 2^n and 2^{n+1} for some n, we find that they occur at cells numbered $(4^j - 1)/3$ and $2(4^j - 1)/3$. The envelope of the eigenvector, that is, the smooth curve through these maxima, is found to increase as a power law with distance: $x_n^{\max} \sim n^{\nu}$. For $R = 0.2$, the exponent was found to be approximately $\nu = 0.227$; for $R = 0.8$, we found $\nu = 0.607$. We see then that the eigenvector exhibits a power law growth from the minimum, or alternatively a power law decrease from the maximum (which for this infinite system lies at infinity). This eigenvector is thus intermediate between an extended state, such as that found for FP1, and an exponentially localized state, such as those found in random systems. Eigenvectors of the type of FP2 are termed "critical."

4.3. Explanation of the Observed Scaling

We may explain the algebraic scaling of the envelope of FP2 using our transfer matrix formalism. Define

$$P_n = x_{(4^{n+1}-1)/3} \qquad \text{and} \qquad Q_n = x_{(4^{n+1}-1)/3-1}$$

Then, since $(4^{n+1}-1)/3 = 2^0 + 2^2 + \cdots + 2^{2n}$, we have

$$\begin{pmatrix} P_n \\ Q_n \end{pmatrix} = M_2 M_4 \cdots M_{2n} \begin{pmatrix} x_1 \\ x_0 \end{pmatrix} \equiv \Lambda_n \begin{pmatrix} x_1 \\ x_0 \end{pmatrix} \tag{4.14}$$

As suggested by the numerical evidence, let us assume a scaling for the peaks such that $\lim_{n\to\infty} P_{n+1}/P_n = \eta$. We may relate η to the exponent ν defined above: $P_n \sim (4^n)^\nu$, and hence $\eta = 4^\nu$. Thus,

$$\nu = \log \eta / \log 4 \tag{4.15}$$

To determine η, we employ the following method. We write

$$\begin{pmatrix} P_n \\ Q_n \end{pmatrix} = \Lambda_{n-1} M_{2n} \begin{pmatrix} x_1 \\ x_0 \end{pmatrix} = \Lambda_{n-1} \begin{pmatrix} x_{2^{2n}+1} \\ x_{2^{2n}} \end{pmatrix} \tag{4.16}$$

But we can calculate this last vector from the transfer matrix (4.12) and the initial conditions (4.13):

$$\begin{pmatrix} x_{2^{2n}+1} \\ x_{2^{2n}} \end{pmatrix} = \frac{1+R-R^2}{1-R} \begin{pmatrix} x_1 \\ x_0 \end{pmatrix} + \left[\frac{2R^{2n}}{1-R} + \frac{R^{2n+1}}{(1-R)^2} \right] \begin{pmatrix} 1 \\ 0 \end{pmatrix} \tag{4.17}$$

Inserting Eq. (4.17) into (4.16), we obtain

$$\begin{pmatrix} P_n \\ Q_n \end{pmatrix} = \frac{1+R-R^2}{1-R} \begin{pmatrix} P_{n-1} \\ Q_{n-1} \end{pmatrix} + \left[\frac{2R^{2n}}{1-R} + \frac{R^{2n+1}}{(1-R)^2} \right] \Lambda_{n-1} \begin{pmatrix} 1 \\ 0 \end{pmatrix} \tag{4.18}$$

Let the components of Λ_n be denoted λ_{ij}^n. For large n, we may write $\eta = P_n/P_{n-1} = P_{n+1}/P_n$. Using Eq. (4.18) to evaluate these two ratios and then equating them, we obtain

$$\begin{aligned} \eta &= \frac{\lambda_{11}^n}{\lambda_{11}^{n-1}} \frac{2R^{2n+2}/(1-R) + R^{2n+3}/(1-R)^2}{2R^{2n}/(1-R) + R^{2n+1}/(1-R)^2} \\ &= \frac{\lambda_{11}^n}{\lambda_{11}^{n-1}} R^2 \end{aligned} \tag{4.19}$$

Now, $\Lambda_n = \Lambda_{n-1} M_{2n}$. Hence, $\lambda_{11}^n/\lambda_{11}^{n-1} = \alpha_{2n} + \gamma_{2n} l_{n-1}$ and $\lambda_{12}^n/\lambda_{11}^{n-1} = \beta_{2n} +$

$\delta_{2n} l_{n-1}$, where $l_{n-1} = \lambda_{12}^{n-1}/\lambda_{11}^{n-1}$. Combining the first of these equations with Eq. (4.19), we obtain

$$l_{n-1} = \frac{1}{\gamma_{2n}} \left(\frac{\eta}{R^2} - \alpha_{2n} \right) \tag{4.20}$$

From Eq. (4.14) we can write η in yet another form. Since $P_n = \lambda_{11}^n x_1 + \lambda_{12}^n x_0$, we have

$$\begin{aligned} \eta &= \frac{\lambda_{11}^n x_1 + \lambda_{12}^n x_0}{\lambda_{11}^{n-1} x_1 + \lambda_{12}^{n-1}} x_0 \\ &= \frac{(\alpha_{2n} + \gamma_{2n} l_{n-1}) x_1 + (\beta_{2n} + \delta_{2n} l_{n-1}) x_0}{x_1 + l_{n-1} x_0} \end{aligned} \tag{4.21}$$

We then insert Eq. (4.20) into Eq. (4.21) and solve the resulting quadratic equation for η. We find the solution (choosing the root that gives $\eta > 1$, as seen numerically)

$$\eta = \tfrac{1}{2}[1 + 2R + (1 + 4R)^{1/2}] \tag{4.22}$$

For $R = 0.2$, Eq. (4.22) gives $\nu = \log \eta / \log 4 = 0.2275...$; for $R = 0.8$, it gives $\nu = 0.6085...$. The numerical results found above are in excellent agreement with these exact values.

4.4. Eigenvectors at Other Points in the Spectrum

The only frequencies we know in the infinite spectrum are those corresponding to lower band edges in the periodic approximations. We expect that the other frequencies iterate to one of the two fixed points, and that thus their corresponding eigenvectors behave similarly to those at the fixed points, although on a different length scale. (It is conceivable that there are frequencies which correspond to chaotic or n-cycle solutions to the renormalization equations, but there is no evidence of this in the numerical data.) We see this length scale expansion explicitly in Fig. 4, where we have plotted the eigenvector corresponding to a lower band edge first appearing in the period-32 system. Note that the eigenvector also has period 32, and is thus simply an inflation of the eigenvector at the first fixed point as seen in Fig. 3a.

5. VIBRATIONAL SPECTRUM. CASE II

5.1. Numerical Results

We now turn to the case where the hierarchy is in the masses, as expressed by Eqs. (2.1) and (2.3). We assume here that $R > 1$; this is done

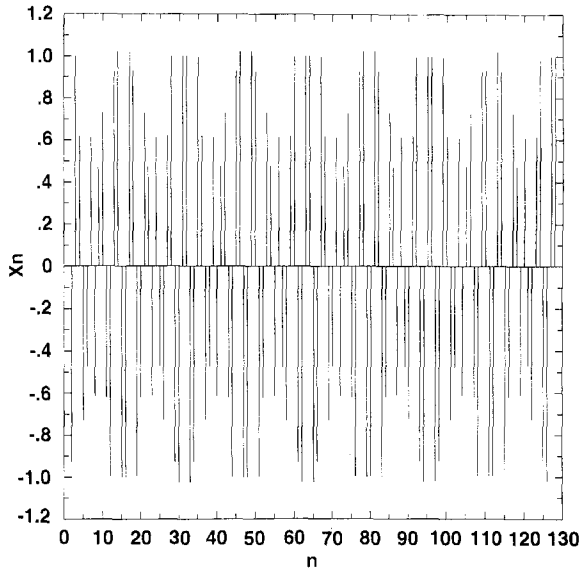

Fig. 4. An eigenvector corresponding to the squared frequency $z = 2.02399569$, in case I. We have used $R = K = 0.5$. This frequency corresponds to the bottom of the 19th band in the period-32 system.

so as to make the problem as similar to case I as possible and to simplify the interpretation of the renormalization group investigation described in the next section. Numerically, we have studied this problem in precisely the same way as was done for case I in Section 3. The allowed frequency bands for several consecutive periods are shown in Fig. 5 for $R = 1.5$ (the general features of the spectrum for this value of R are representative of those for any other value). First, we observe that for any given period p_n, the total bandwidth B_n is given by

$$B_n = 4/R^n \tag{5.1}$$

Thus, once again the picture of the band structures for a sequence of systems of increasing period, as shown here in Fig. 5, shows explicitly the construction of the zero-measure Cantor set spectrum in the infinite limit.

As in case I, we have investigated the scaling properties of the spectrum in great detail. After examining many different R and p_n values, we again find that the spectrum is governed by only two scaling parameters, of precisely the same description as above: the first gives the limiting ratio of the width of any band in the period-p_n system to that of the lower band into which it splits in the period-p_{n+1} system; the second describes the ratio to that of the upper band into which it splits. As numerical examples, we find for $R = 1.5$ that $\lambda_1 = 4.07$ and $\lambda_2 = 5.41$; for $R = 4$, we find $\lambda_1 = 8.03$ and $\lambda_2 = 9.94$; and for $R = 8$, we obtain $\lambda_1 = 16.0$ and $\lambda_2 = 17.3$.

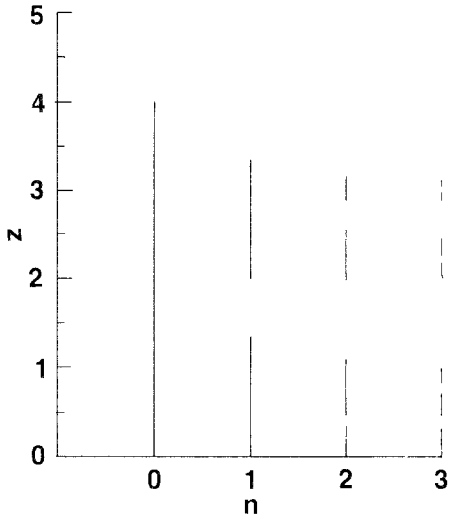

Fig. 5. The allowed frequency bands (in dimensionless units) in case II for periodic systems of period 2^n, $n=0, 1, 2, 3$. We have used $R=M_1=1.5$ and $M_2=0$.

We may also carry out the calculation of the fractal dimension following the same arguments as in Section 2, except this time using Eq. (5.1). Doing so leads to

$$D_0=\log 2/\log(2R) \tag{5.2}$$

For $R=1$, this gives a fractal dimension $D_0=1$, in agreement with the band structure implied by Eq. (2.4). For $R\to\infty$, Eq. (5.2) gives a fractal dimension $D_0=0$. This corresponds to the case where every other mass is infinitely large. Hence, the spectrum consists of the single point $z=2$, which clearly has fractal dimension zero.

Lastly, we again note that the lower band edges for the period-p_n system remain in the band structure of all larger-period systems, and hence the infinite system as well. The explanation for this effect is the same as in case I (see the end of Section 3.2), this time using the renormalization equations, which we derive in the next section.

5.2. Renormalization Group Analysis

We may account for the scaling properties of the spectrum through a renormalization procedure analogous to that in Section 3. Decimate all the odd-site masses, as shown in Fig. 1b, and obtain

$$x_{2n+1}=\frac{x_{2n+2}+x_{2n}}{2-\mu_0 z} \tag{5.3}$$

Let us consider the five sites labeled 0, 1,..., 4 in Fig. 1b. The equation of motion for the second mass is

$$-\mu_1 z x_2 = x_3 + x_1 - 2x_2 = \frac{x_4 + 2x_2 + x_0}{2 - \mu_0 z} - 2x_2 \tag{5.4}$$

We may rewrite this in a form analogous to the original,

$$-\mu_0' z' x_{1'} = x_{2'} + x_{0'} - 2x_{1'} \tag{5.5}$$

provided that we define

$$\begin{aligned} z' &= (z/\mu_0)[\mu_1(2 - z\mu_0) + 2] \\ \mu_0' &= \mu_0 \\ x_{n'} &= x_{2n} \end{aligned} \tag{5.6}$$

Next, we need to consider how the other mass values should be renormalized. Consider the mass $m_0 = \mu_k$ for some k. The basic equation of motion reads $-\mu_k z x_0 = x_{-1} + x_1 - 2x_0$, which when rearranged can be written

$$\left(2 - \frac{4}{2 - z\mu_0} - \mu_k\right)(2 - z\mu_0)\, x_0 = x_2 + x_{-2} - 2x_0 \tag{5.7}$$

We may thus write this equation in the form

$$-\mu_{k-1}' z' x_{0'} = x_{1'} + x_{-1'} - 2x_{0'}$$

provided that Eq. (5.6) holds and that

$$\mu_{k-1}' = \mu_0 \frac{2\mu_0 + \mu_k(2 - z\mu_0)}{2\mu_0 + \mu_1(2 - z\mu_0)}, \qquad k \geqslant 1 \tag{5.8}$$

[The condition at $k = 1$ agrees with Eq. (5.6).]

We now generalize our original definition of the masses, Eq. (2.3), so as to obtain a closed renormalization scheme. Define

$$\mu_k = \begin{cases} 1, & k = 0 \\ M_1 R^{k-1} + M_2, & k \geqslant 1 \end{cases} \tag{5.9}$$

If $M_1 = R$ and $M_2 = 0$, we recover our original definition. The renormalized masses given by Eq. (5.8) will have the form of Eq. (5.9) provided we define renormalized values M_1' and M_2' such that

$$M_1' = \frac{RM_1(2-z)}{2+(M_1+M_2)(2-z)}$$
$$M_2' = \frac{2+M_2(2-z)}{2+(M_1+M_2)(2-z)} \tag{5.10}$$

In terms of M_1 and M_2, we may write the renormalization equation for z as

$$z' = [2+(M_1+M_2)(2-z)] \tag{5.11}$$

Equations (5.10) and (5.11) form the basis for the renormalization group treatment. Let us consider the fixed points of these equations. We find that there are four fixed points, namely

$$\begin{aligned}
&z^{(1)*}=0, && M_1^{(1)*}=R\frac{2-R}{1-R}, && M_2^{(1)*}=\frac{-1}{1-R}\\
&z^{(2)*}=\frac{2R-1}{R}, && M_1^{(2)*}=R\frac{1+R}{1-R}, && M_2^{(2)*}=\frac{-2R}{1-R}\\
&z^{(3)*}=0, && M_1^{(3)*}=0, && M_2^{(3)*}=1\\
&z^{(4)*}=3, && M_1^{(4)*}=0, && M_2^{(4)*}=1
\end{aligned} \tag{5.12}$$

To interpret the relevance of each fixed point, we again consider the infinite system as a periodic one for some large period p_n. After renormalizing n times, we map the original system into the example we considered in Section 2. There we found that a frequency is in the spectrum provided that $z \in [0, 4]$. Thus, in this problem, a frequency z is in the infinite system if and only if its n-times renormalized value $z^{(n)} \in [0, 4]$. For the fixed points, this imlies that points which iterate to them are in the spectrum if and only if the corresponding $z^* < 1$. From Eq. (5.12), for $R > 1$, we see that all four fixed points are relevant in this sense.

Let us next consider the stability and scaling properties of the fixed points. Diagonalizing the matrix $[\partial(z', M_1', M_2')/\partial(z, M_1, M_2)]$, we find that the maximum eigenvalues (for $R > 1$) are

$$\begin{aligned}
\lambda_{\max}^{(1)} &= 2R\\
\lambda_{\max}^{(2)} &= \frac{1}{2R}\{(1+2R+2R^2)+[(1+2R+2R^2)^2-8R]^{1/2}\}\\
\lambda_{\max}^{(3)} &= \begin{cases} 4, & R<8 \\ R/2, & R>8 \end{cases}\\
\lambda_{\max}^{(4)} &= \begin{cases} 2, & R<2 \\ -R, & R>2 \end{cases}
\end{aligned} \tag{5.13}$$

Note that once again all the fixed points are repulsive, as required by the zero measure of the spectrum. From close scrutiny of the numerical results, it is apparent that for $R \in [1, 2]$, points near the bottom of any band iterate toward the third fixed point before deviating, while those near the tops of bands iterate toward the second fixed point. For $R > 2$, we find that points near the bottom iterate toward the first fixed point, while those near the top still iterate toward the second. For no value of R does the fourth fixed point appear to play a role. The reason for this is not clear; since $z^{(4)*} \in [0, 4]$, we might expect it to be relevant.

The scaling properties observed in Section 5.1 are now easy to see. The scaling near the bottom of the bands is determined by fixed points one and three; that near the top is determined by fixed point two. For $R = 1.5$, we have $\lambda_{\max}^{(3)} = 4$ and $\lambda_{\max}^{(2)} = 6.3423...$; for $R = 4$, we have $\lambda_{\max}^{(1)} = 8$ and $\lambda_{\max}^{(2)} = 10.200...$; for $R = 8$, we get $\lambda_{\max}^{(1)} = 16$ and $\lambda_{\max}^{(2)} = 18.111...$. The numerical results in Section 5.1 agree well with these exact values.

6. THERMODYNAMIC PROPERTIES

We consider now applications of the above formalism to the calculation of the low-frequency integrated density of states and the low-temperature heat capacity. Define $H(z)$ to be the fraction of vibrational states with squared frequency less than z. For either case I or II, we let x_n be the z value of the top edge of the bottom band in the period $p_n = 2^n$ system. From Sections 3 and 5, we know that $x_n \sim \lambda^{-n}$, where λ is the appropriate scaling value for the lowest band. But we also know that $H(x_n) = 2^{-n}$, since each band has the same number of states and there are 2^n total bands in the period-p_n system. Hence, in the limit $z \to 0$, we have

$$H(z) \sim z^{\log 2/\log \lambda} \equiv z^{\beta} \tag{6.1}$$

where for case I, β is given by

$$\beta = \begin{cases} \log 2/\log(2R), & 0 < R < 1/2 \\ 1/2, & 1/2 < R < 1 \end{cases} \qquad \text{(case I)} \tag{6.2}$$

and for case II

$$\beta = \begin{cases} 1/2, & 1 < R < 2 \\ \log 2/\log(2R), & R > 1/2 \end{cases} \qquad \text{(case II)} \tag{6.3}$$

We may use this information about the integrated density of states to calculate the low-temperature specific heat. As a function of the frequency ω, $H(\omega) \sim \omega^{2\beta}$, implying that the density of states $N(\omega) = dH/d\omega \sim \omega^{2\beta - 1}$.

For the harmonic chain the energy $\varepsilon \propto \omega$, and hence $N(\varepsilon) \sim \varepsilon^{2\beta - 1}$. The heat capacity is then

$$C \sim \frac{\partial}{\partial T} \int d\varepsilon \, N(\varepsilon) \frac{\varepsilon}{e^{\varepsilon/k_B T} - 1} \sim T^{2\beta} \tag{6.4}$$

Note that as $R \to 1$, in either case I or II, we recover the normal one-dimensional result $C \sim T$. For other values of R, however, we obtain an anomalous exponent dependent on the parameter R describing the hierarchy. In particular, for an appropriate value of R, we may obtain an exponent on the heat capacity anywhere in the interval [0, 1].

Furthermore, from the form of the exponent β given in Eqs. (6.2) and (6.3), we see that there is a singularity in the specific heat as a function of R. The presence of this singularity is reminiscent of another such one found in studying diffusion in a system with a hierarchical array of transition rates—the ultradiffusion problem.[2,5] In fact, there is a close analogy between the diffusive system and the vibrational one studied here, for case I. Alexander and Orbach[18] have shown that

$$d_s = 2d_f/d_w \tag{6.5}$$

where $d_s = 2\beta$ is the spectral dimension, d_f is the fractal dimension of the underlying lattice, and d_w is the random walk dimension for the diffusion problem defined by $\langle r^2(t) \rangle \sim t^{2/d_w}$. In our case, we have $d_f = 1$. From the study of ultradiffusion, we knowq that $2/d_w = 2 \log 2/\log(2R)$, $0 < R < 1/2$, and $2/d_w = 1$ for $1/2 < R < 1$. Hence, the expression for β predicted by Eq. (6.5) agrees exactly with that derived in Eq. (6.2). The underlying dynamical properties of the diffusion and vibrational problems are thus completely related by Eq. (6.5).

We may also relate our hierarchical problem to that of vibrations in a random system. To be explicit, consider case I, and let $\rho(k)$ be the density of spring constant values. Since a fraction 2^{n+1} of the springs have value $k_n = R^n$, we see that $\rho(k) \sim k^{-\alpha}$, where $\alpha = \log(2R)/\log(R)$. If we now consider a *random* system with the same density of spring constants, we find[12] that the expressins for the low-frequency density of states and low-temperature specific heat are precisely the same as found above. Furthermore, we know that the random vibrational problem is related to the random diffusion problem, again through Eq. (6.5). Therefore, there is a close relationship among all four problems, which we have depicted in Fig. 6.

We may exploit the relationship of hierarchical vibrations to ultradiffusion by anticipating the results of the vibrational problem in higher dimensions.[5] If we consider a cubically arranged array of springs in masses in d dimensions, we will still have a fractal dimension $d_f = 1$ (our set

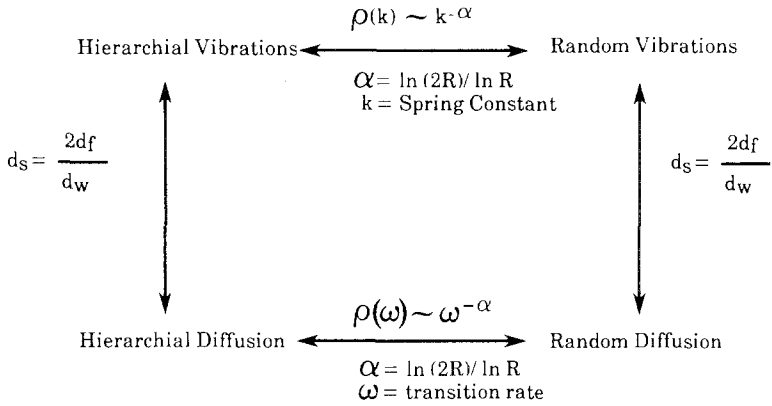

Fig. 6. A schematic representation of the relationship among the four problems—hierarchical diffusion and vibration, and random diffusion and vibration—discussed in Section 6.

is simply a union of line segments of dimension one). The random walk dimension $2/d_w$, however, increases by a factor of d. Hence, from Eq. (6.5), we anticipate that the spectral dimension in d dimensions is $d_s^{(d)} = d \cdot d_s^{(1)}$. This gives a value for the exponent $\beta^{(d)}$ in case I of

$$\beta^{(d)} = d\beta = \begin{cases} d \log 2/\log(2R), & 0 < R < 1/2 \\ d/2, & 1/2 < R < 1 \end{cases} \tag{6.6}$$

Because $\beta^{(d)}$ can assume any value in $[0, d/2]$ for an appropriate R value, this might lead to an ambiguity in the physical origin of the power law behavior in the specific heat at low temperatures. For example, in three dimensions, the electronic specific heat is linear in T at low temperatures. If one observed such a linear behavior in a hierarchical system where $\beta^{(3)}(R) = 1/2$, it would be unclear if the effect were due to the electronic or the vibrational properties.

7. SUMMARY

In this paper we have considered the vibrational properties of one-dimensional hierarchical systems. We have discovered that the allowed frequency spectrum forms a zero-measure Cantor set and that the corresponding eigenvectors are either extended or self-similar and critical. We have employed renormalization group analyses to calculate the scaling properties of the spectra and have verified the results through extensive numerical study. From knowledge of the scaling properties of the spectrum

near zero frequency, we were able to calculate the low-frequency behavior of the density of states and the low-temperature behavior of the specific heat. In the latter, we found a singularity in the exponent as a function of R. In addition, we have exhibited a close relationship between these systems and the hierrchical diffusion problem, as stated in Eq. (6.5), and with the random diffusion and vibration problems. For random systems, we find that results are identical to the hierarchical ones provided that we take the density of spring constants (or masses) equal to that of the hierarchical system.

ACKNOWLEDGMENTS

This work was supported in part by the U. S. Office of Naval Research, contract N00014-82-0699. One of the authors (H.A.C.) is supported by CONICET of Argentina. We would like to thank the referee for noting an improved method for deriving Eq. (4.5).

REFERENCES

1. B. A. Huberman and M. Kerszberg, *J. Phys. A* **18**:L331 (1985).
2. S. Teitel and E. Domany, *Phys. Rev. Lett.* **55**:2176 (1985).
3. A. Maritan and A. L. Stella, *J. Phys. A* **18**:L269 (1986).
4. S. Teitel, D. Kutasov, and E. Domany, *Phys. Rev. B* **36**:684 (1987).
5. W. P. Keirstead and B. A. Huberman, *Phys. Rev. A* **36**:5392 (1987).
6. T. Schneider, D. Würtz, A. Politi, and M. Zannetti, *Phys. Rev. B* **36**:1789 (1987).
7. H. E. Roman, *Phys. Rev. B* **36**:71 (1987).
8. R. Livi, A. Maritan, and S. Ruffo, preprint (1987).
9. H. A. Ceccatto, W. P. Keirstead, and B. A. Huberman, *Phys. Rev. A* **36**:5509 (1987).
10. H. A. Ceccatto and W. P. Keirstead, *J. Phys. A* **21**:L75 (1988).
11. F. Dyson, *Phys. Rev.* **92**:1331 (1949).
12. S. Alexander, J. Bernasconi, W. R. Schneider, and R. Orbach, *Rev. Mod. Phys.* **53**:175 (1981), and references therein.
13. J. M. Luck and D. Petritis, *J. Stat. Phys.* **42**:289 (1986).
14. M. Kohmoto and J. R. Banavar, *Phys. Rev. B* **34**:563 (1986).
15. B. A. Huberman and T. Hogg, *Physica* **22D**:376 (1986).
16. C. P. Bachas and B. A. Huberman, *Phys. Rev. Lett.* **57**:1965 (1986); *J. Phys. A* **20**:4995 (1987).
17. H. A. Ceccatto and B. A. Huberman, *Physica Scripta* **37**:145 (1988).
18. S. Alexander and R. Orbach, *J. Phys. (Paris) Lett.* **43**:L625 (1982).